J Mater Sci

Metals & corrosion

Promising elastocaloric properties of sintered polycrystalline NiMnGa produced by open die pressing

Francesca Villa[1,2,*], Michela Tamandi[3], Francesca Passaretti[1], Enrico Bassani[1], and Elena Villa[1]

[1] *National Research Council, Institute of Condensed Matter Chemistry and Technologies for Energy (CNR-ICMATE), Lecco, Italy*
[2] *Department of Mechanical Engineering, Politecnico di Milano, Milan, Italy*
[3] *Material Science Department, Università di Milano-Bicocca, Milan, Italy*

Received: 30 June 2023
Accepted: 20 September 2023

ABSTRACT

The increasing interest in the development of multicaloric materials for solid-state cooling applications is giving rise to the investigation of elastocaloric performance of ferromagnetic Shape Memory Alloys (FeSMA). Moreover, some sintering processes have been proposed to overcome the well-known brittleness of these alloys. In this context, a novel application of the open die pressing (ODP) method for the preparation of NiMnGa polycrystalline samples sets the chance to have interesting mechanical properties, until now never reported in literature. In this work, a tunable optimization of microstructure is presented and the elastocaloric properties are investigated by different mechanical approaches and direct measurement of adiabatic ΔT values. It is observed, for the first time, a polycrystalline NiMnGa alloy that exhibits an extremely stable mechanical and thermal response upon 200 adiabatic compression cycles. The best performance consisted in a ΔS peak of 35 J/(kg °C) and an adiabatic ΔT value of ± 4 °C in the first 10 cycles and + 3,75 / − 4 °C in stabilized conditions over 200 cycles.

Introduction

The exploration of novel sustainable and efficient refrigeration and heat pumping technologies to replace the traditional methods based on vapour compression, is becoming a key issue in recent years. Solid-state caloric refrigeration, including elastocaloric cooling, has proven to be a valuable and significant alternative to the traditional technologies [1, 2]. Moreover, the research has been successfully devoted to the study and the characterization of the caloric materials [3] and to the development of efficient and eco-friendly cooling system prototypes at the small and large scale [4–6]. Currently, only few elastocaloric demonstrators and prototypes have been developed, but this

Handling Editor: Megumi Kawasaki.

Address correspondence to E-mail: francesca.villa@icmate.cnr.it

E-mail Addresses: m.tamandi@campus.unimib.it; francesca.passaretti@cnr.it; enrico.bassani@cnr.it; elena.villa@cnr.it

https://doi.org/10.1007/s10853-023-08977-4
Published online: 05 October 2023

technology is designated to become one of the most promising alternative cooling methods.

When an external field is adiabatically applied to caloric materials, they exhibit a change in temperature which is reversible upon the field release [7]. Among caloric materials, the shape memory alloys (SMAs) are one of the most promising candidates since the applied external field (magnetic, mechanical or electric) induces a significant entropy change and a related reversible thermal reaction [8, 9]. These caloric effects can be described by two parameters, i.e., the total change of temperature in adiabatic conditions (ΔT_{ad}) and the total change of entropy in isothermal conditions (ΔS_{iso}). In addition, a coefficient of performance (COP) can be evaluated [7, 10].

Superelastic SMAs are the most promising candidates for the elastocaloric cooling since the applied mechanical stress induces a reversible solid-state transition, i.e., the stress-induced martensitic transformation. Particularly, among the SMAs, the most efficient caloric materials are NiTi [11, 12] and NiMnTi alloys [13, 14]. Their caloric performances in terms of ΔT_{ad}, ΔS_{iso} and COP are well-established, with values of ΔT_{ad} up to 25 and 30 °C, respectively.

On the other hand, the ferromagnetic SMAs (FeSMAs) are mainly studied for their magnetic properties [15, 16] and magnetocaloric effect [17, 18]. A lower number of studies are devoted to the investigation of the elastocaloric properties of the FeSMAs due, principally, to the intrinsic brittleness typical of these alloys. Among the FeSMAs, NiMnGa- and NiMnGa-based systems are the most studied ones for their magnetocaloric properties. However, some elastocaloric investigations could be found in literature in view of the magneto-elastic coupling for multicaloric applications [19, 20]. In these studies, only few elastocaloric cycles in compressive configuration were possible on cast NiMnGa samples.

In order to decrease the brittleness of NiMnGa, starting from previous experience with powders processing [21], an alternative production method, namely, the open die pressing (ODP), was developed [22] and dense samples with a highly elastic response were produced. So far, a complete characterization of the thermo-mechanical properties of these sintered samples was provided. In the present study, the elastocaloric properties of sintered NiMnGa were evaluated in terms of ΔT_{ad} and ΔS_{iso} for the first time. The increased elastic response of the samples produced by means of ODP process allowed a more stable elastocaloric performance with respect to the cast alloy reported in literature. Indeed, the main innovative outcome of this research are the promising elastocaloric properties in terms of ΔT_{ad} and ΔS_{iso} of sintered NiMnGa samples under several elastocaloric cycles in view of multicaloric applications.

Materials and methods

The sintering process of this work starts from powders prepared by a planetary ball milling equipment. For this milling process, some ingots of $Ni_{50}Mn_{30}Ga_{20}$ (at%) were prepared by arc melting using pure elements of minimum 99,97% in purity. The alloy was prepared after 5 cycles of re-melting to ensure a good homogeneity of the material. The size of the powders obtained was selected by sieves and regulated in dimension lower than 50 μm.

For this activity, we refer to open die pressing process described in our previous work [22]. We use the same runs to prepare dense samples, by closing the powders in iron sheath and by pressing in two steps at 700 °C under 40 tons for 30″ and at 500 °C under 10 tons for 10′. The preparation ends with cooling down the sample by slow cooling or water quench. During this process, the powder's rearrangement, densification, sintering and finally consolidation of the grain structure with high density quite near to cast material takes place.

Smaller different kind of specimens have been cut from ODP samples for the various experimental tests. The as-processed samples were labeled as "ODP_AP". The ODP samples that were subjected to thermal treatments at 925 °C for 6 and 24 h followed by WQ water quench or SC slow cooling were labeled respectively as ODP1_6h, ODP1_24h (WQ) and ODP2_6h, ODP2_24h (SC).

The control of the density of the ODP samples was performed by Archimedes method on 10 consecutive measures.

Instron E3000 Dynamic Mechanical test machine with thermal chamber temperature control equipment, with liquid nitrogen cooling system, was used for mechanical investigation in compression configuration. Two series of tests have been carried out: (1) SR strain recovery test under fixed stress vs temperature and (2) SS stress strain measure at isothermal condition.

The tests (1) were performed with a change temperature rate of 5 °C/min and in the [25 °C; 300 °C] temperature range. For these tests, an accurate control of the base line and the real thermal deviation from rate imposed and the deformation due to thermal dilatation of the system was applied. From these data, by elaboration through Maxwell equation [23], we obtained the ΔS change value in cooling and heating step.

The test (2) were registered at constant temperature and with compression stress-rate of 5 MPa/min until 400 MPa. The elastocaloric characterization was indeed performed in strain control up to strains between 2,5 and 3,5% at rates between 300 and 400%/min to approach the adiabatic conditions. The holding period of 70 s between the loading and unloading phase is considered to avoid heat retain in the sample. An ad hoc experimental set up developed in our laboratory allowed the direct measurement of the ΔT data, by means of T-type thermocouples. The thermocouples were connected to an acquisition system (NI 9212 thermocouple input module for National Instruments CompactDAQ) which allowed the high-frequency acquisition of the thermal signal ΔT elaborated by LabVIEW program.

Result

The ODP method allowed to obtain samples with a density of 7.7 g/cm^3 and this value corresponds to a relative density of 96.5% with respect to the value measured for the cast alloy, i.e. 8 g/cm^3. A level of porosity corresponding to 3.5% is good for sintered samples and makes them comparable to the cast ones.

The results of the calorimetric analysis are reported in previous work [22] and the principal information about the TMT (Thermoelastic Martensitic Transformation) are resumed in Table 1. The principal aspects observed from the thermal analysis are the high thermal cycling stability and the shift to higher temperatures, the narrowing and the increase in the enthalpies of the peaks related to the TMT and reverse transformation for the thermally treated samples with respect to the as-processed ones.

The strain recovery tests showed the deformation behavior of the ODP samples upon temperature change under constant compressive loads. It is possible to observe that in correspondence of the TMT, both upon cooling and heating, there is a deflection of the curves. During cooling the absolute strain value increases, while upon heating the absolute strain decreases. The strain recovery curves under fixed stresses versus temperature are reported in Fig. 1, and in addition, both the maximum recovered strain and the residual strain for all the samples are reported in the graphs in Fig. 2.

Table 1 Differential scanning calorimetry (DSC) related data for as-processed and thermally treated ODP samples

Sample	Af (°C)	ΔH (J/g)
ODP1_AP	111,8	3,4
ODP1_6h	130,4	7,0
ODP1_24h	136,3	8,7
ODP2_AP	110,0	2,4
ODP2_6h	129,9	6,8
ODP2_24h	125,0	8,4

These series of curves are important to describe the mechanical behavior of the material related to phase transformation. The measurements were performed under different stress values and, for sake of simplicity, only the most significant curves are reported in Fig. 1. The samples of the series 1 are able to withstand a wider range of applied stresses, while some samples of series 2 displayed under high loads the formation of cracks and ruptures that hindered a significant signal of strain. Generally, the samples thermal treated for 6h exhibits the best performances, and in particular, the ODP1_6h sample presents the best behavior in terms of recovered strain and the lowest residual strain.

The elaboration of the strain recovery curves by means of Maxwell Equation [23] led to the evaluation of the entropy variation in correspondence of the TMT upon cooling and heating and the results are reported in Fig. 3. The highest values of ΔS are reached by the sample of series 1 which developed more defined strain recovery curves with sharper slope changes in correspondence of the TMT. ΔS maximum values of 24 and 35 J/(kg °C) were obtained upon heating for samples ODP1_6h and ODP1_24h respectively in correspondence of applied loads of 260 MPa. Despite higher entropy change values, the sample ODP1_24 h shows less coherent and regular curves as is already visible from the curves of Fig. 1.

A series of linear loading–unloading measurements in compression configuration were carried out at different temperatures, to investigate the mechanical behavior of the ODP samples both in austenitic

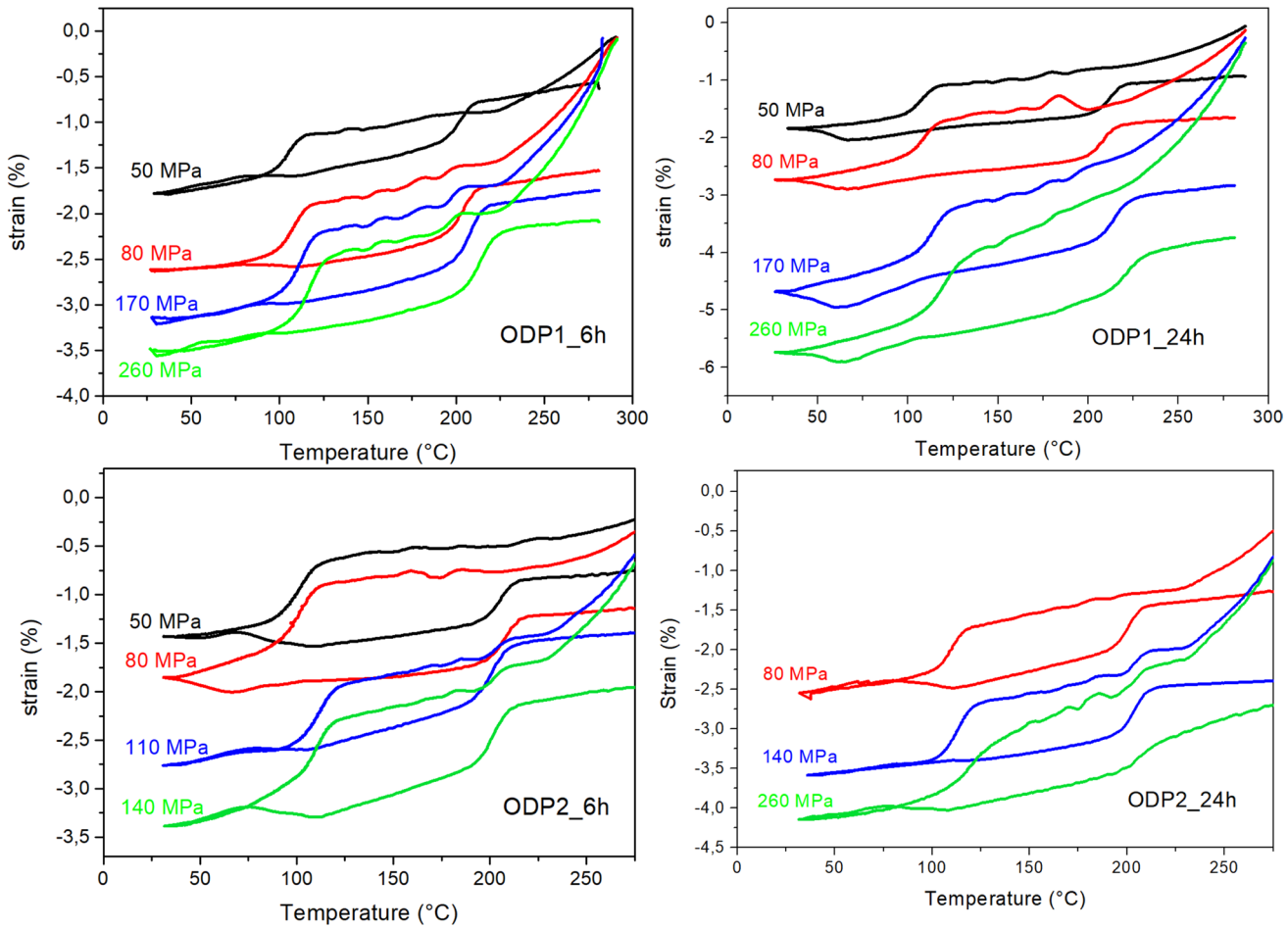

Figure 1 Strain recovery curves under fixed stress vs T, for all the investigated samples.

and martensitic state and the possibility to obtain phase diagrams from stress–strain curves. Figure 4 shows the most representative curves for the martensitic and austenitic behavior (registered at M_f—20 °C and A_f + 10 °C, respectively) under increasing stress for all the samples and in the inset the elastic modulus (E) trend is reported for Martensite and Austenite phases. Elastic moduli were determined by the slope of the tangent line in correspondence of the initial elastic part of the loading curves. The martensite curves show the usual detwinning phenomenon but it is noticeable that this process does not occur at almost constant stress and that there is an important elastic recovery with small residual strain, particularly for samples of series 2. In a similar way, also in austenitic phase the stress induction of martensite is not correspondent to a flat plateau. The shape of the curves is influenced by the strongly elastic and quite linear behavior of these sintered samples, with very small hysteresis loop in austenite. Moreover, for all the samples except ODP2_24h in parent austenitic phase, there is an anomalous recovery of strain until negative values. In addition, the inflection points during the loading stage reveal the critical stresses for the induction of martensite in the austenitic samples, but, due to the particular slope of these curves, it is not possible to individuate them with sufficient precision in all curves. Therefore, a critical stress vs temperature phase diagram is not obtained from stress–strain analysis. Nevertheless, it is possible to have this indication again from the strain recovery curves. It was possible to determine the average temperature of martensitic transition, defined as $(M_s + M_f)/2$, by the identification of the inflection points of each strain recovery curve corresponding to different applied stresses. Figure 5 shows the evaluation of the average transition temperatures in relation to the applied stresses

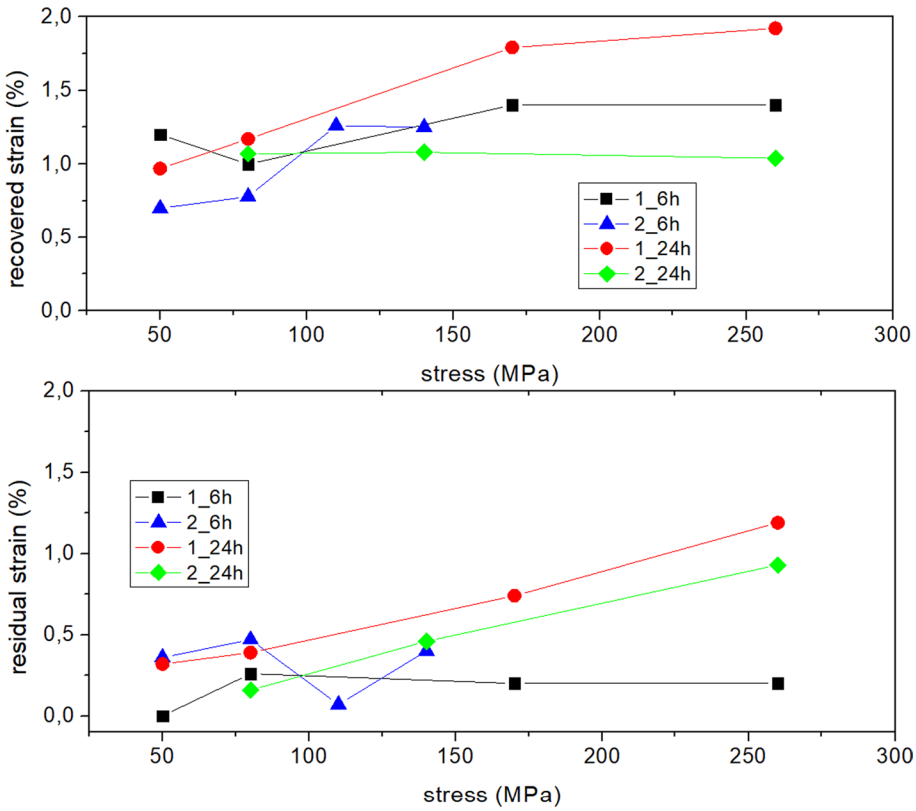

Figure 2 Recovered strain and residual strain data vs applied stress for all the investigated samples.

and the Clausius–Clapeyron coefficients (Kcc) that were determined as the slope of the trend lines are reported.

Finally, from these series of curves it interesting to note that sample ODP1_6h exhibits the highest values of Elastic modulus, the highest difference in modulus values for Austenite and Martensite phases and the highest value for Clausius–Clapeyron coefficient. Generally, it is not wrong to consider that the Kcc for all the samples obtained by ODP process is higher of the usual data reported in literature for the NiMnGa system (about 5 MPa/°C) [24] and this confirms the stronger mechanical properties highlighted in all the experimental characterization.

The elastocaloric study of the ODP sintered samples was completed with direct adiabatic ΔT measurements. The thermocouples setup developed for the direct ΔT measurements allowed the simultaneous recording of the mechanical and thermal signal during adiabatic loading and unloading cycles. Figure 6 resumes the best results obtained from ΔT measurements performed at different rates of deformation and up to different strains. As reported in the figure, the most suitable experimental conditions were correspondent to compression strain of 2.5% and rate of deformation of 300%/min. The maximum ΔT measured for 10 adiabatic cycles performed with these conditions is about 4 °C upon loading and − 4.5 °C upon unloading for sample ODP1_6h.

For the most promising sample, i.e. ODP1_6h, a higher number of cyclic tests was performed, in order to have a first indication of the fatigue performance of the sintered alloy. It is possible to observe in Fig. 7 that at after 200 cycles the ΔT stabilizes to values ranging from 3,75 and 4 °C upon loading and heating without failure of the sample or a drop of the material response. This is a new and interesting result for NiMnGa alloy, since it is not possible to find in literature examples of polycrystalline and non-textured samples that can withstand such number of compressive adiabatic cycles and that has a significantly stable response after several cycles. In this case, the elastocaloric performance in terms of ΔT settles to a value similar to previous ones presented in literature, but it is obtained in promising fatigue conditions.

Finally, it is possible to evaluate the elastocaloric properties of these materials in an indirect way, from a theoretical thermodynamic point of view, as reported in [25–27]. For sake of simplicity, this theoretical evaluation was considered only for the most interesting and

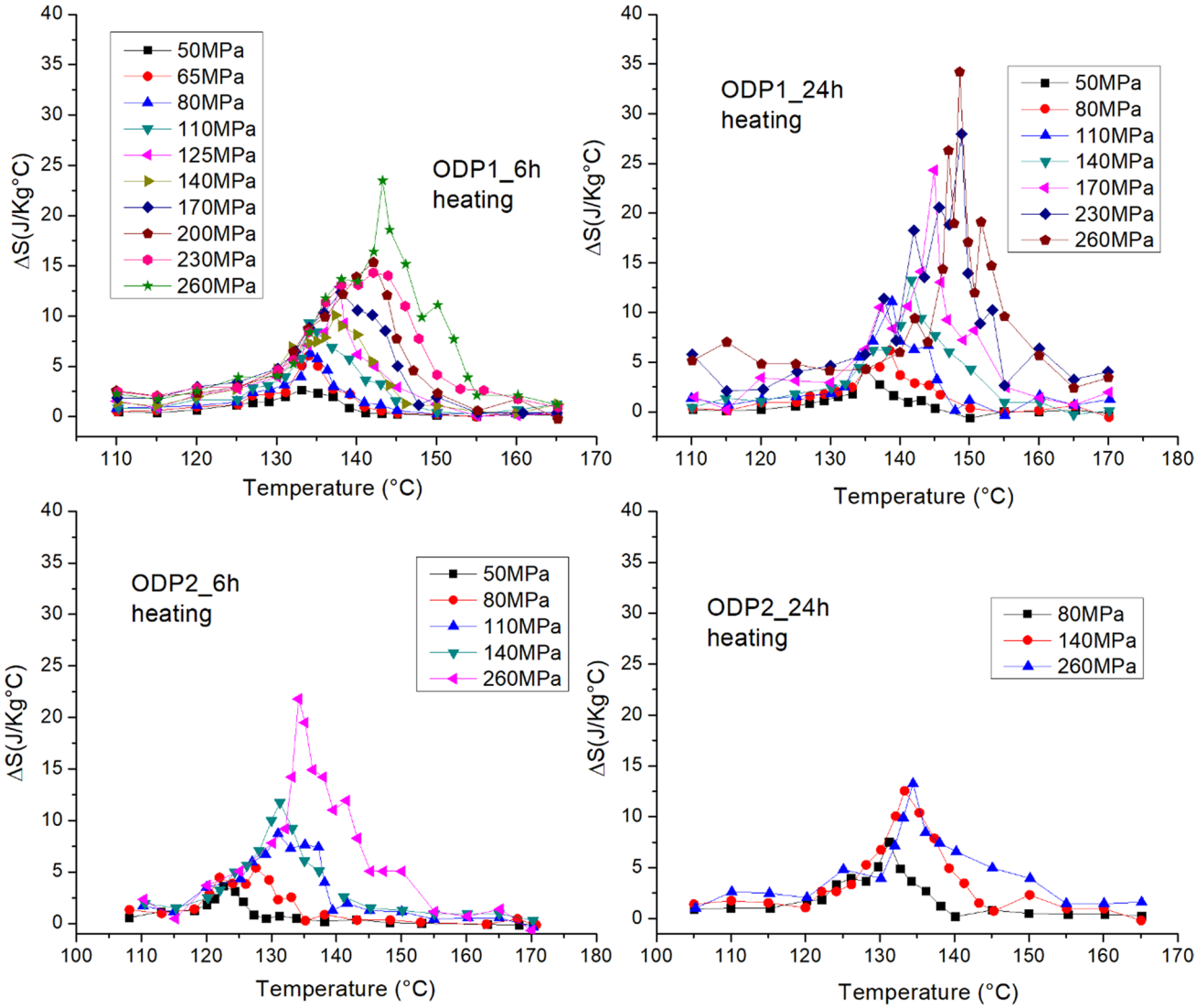

Figure 3 ΔS curves in heating elaborated from strain recovery curves of Fig. 1.

performing sample, i.e. ODP1_6h. Table 2 summarizes the values of ΔT and ΔS for sample ODP1_6h computed starting from the calorimetric data and the Clausius–Clapeyron relation obtained from strain recovery curves. In both cases, the theoretical ΔT and ΔS values obtained are higher than the experimental ones.

Discussion

The use of ODP process to obtain polycrystalline samples of NiMnGa revealed, in our previous work, [22] particular and interesting mechanical performance, in specimens tested in flexural conditions. In this work, the compression configuration was adopted to carry out a complete elastocaloric characterization of NiMnGa sintered alloy. Also in this case is evident that the mechanical performance of these samples is significantly improved with respect to the cast alloy and it allows an efficient elastocaloric effect for a FeSMA. Considering this, it is important to say that the optimization of the elastocaloric response of these alloys is the first step toward the development of multicaloric materials that combine the magnetic and elastic response.

As reported in [22], the ODP process seems to introduce in the material pinned residual strain that is related to stored mechanical energy. This effect is partially re-organized in thermally treated samples, but it is never completely removed. Starting from the

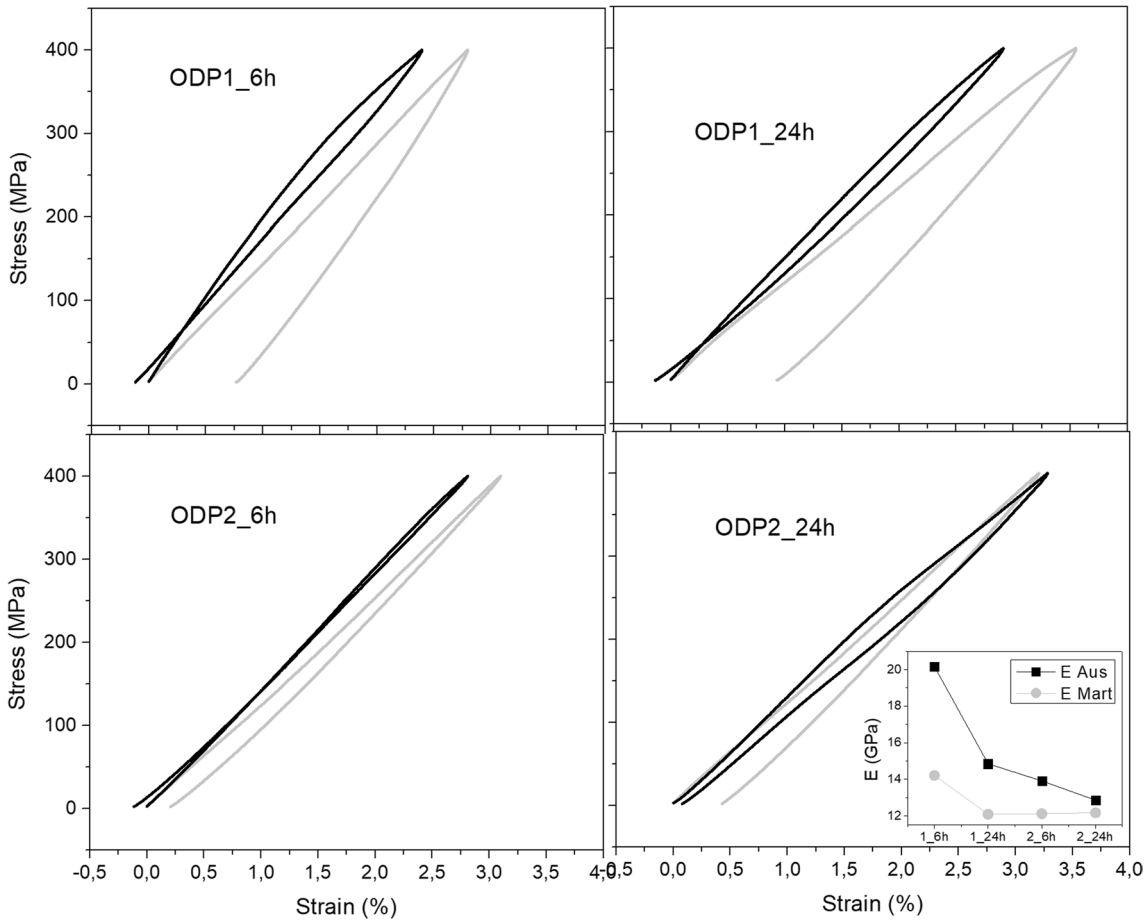

Figure 4 stress–strain curves registered at M_f−20 °C (grey curves) and A_f+10 °C (black curves). The inset shows the values of Elastic Modulus in Austenite and Martensite for all the samples.

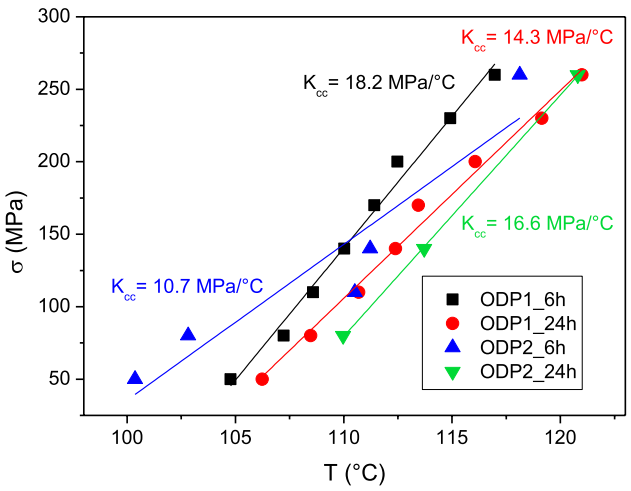

Figure 5 Applied stress vs average martensitic transition temperature evaluated from strain recovery curves and Clausius–Clapeyron (Kcc) coefficient obtained as the slope of the linear fit of the σ vs T points.

strain recovery measurements, this particular microstructural condition leads to an inverse behavior in flexural condition, similar to that observed for melt spun ribbons [28, 29]. In the compression tests carried out in the current work and reported in Fig. 1, the elastic response of the material caused by the dispersion of stored mechanical energy reduces the total strain recovered, increases the stress to observe induction of martensite and reduces the residual strain (as highlighted in Fig. 2). The residual strain of NiMnGa ODP samples reaches values lower than 0.2%, particularly for sample ODP1_6h. Moreover, for this sample the strain recovery curve at the lowest stress (50 MPa) shows, in the recovery ramp upon heating, a beginning of inverse behavior indicated by the crossing with the cooling curve. This trend could be ascribed to a release of mechanical energy that gives a recovery which is higher than the strain induced. In the stress–strain measurements reported

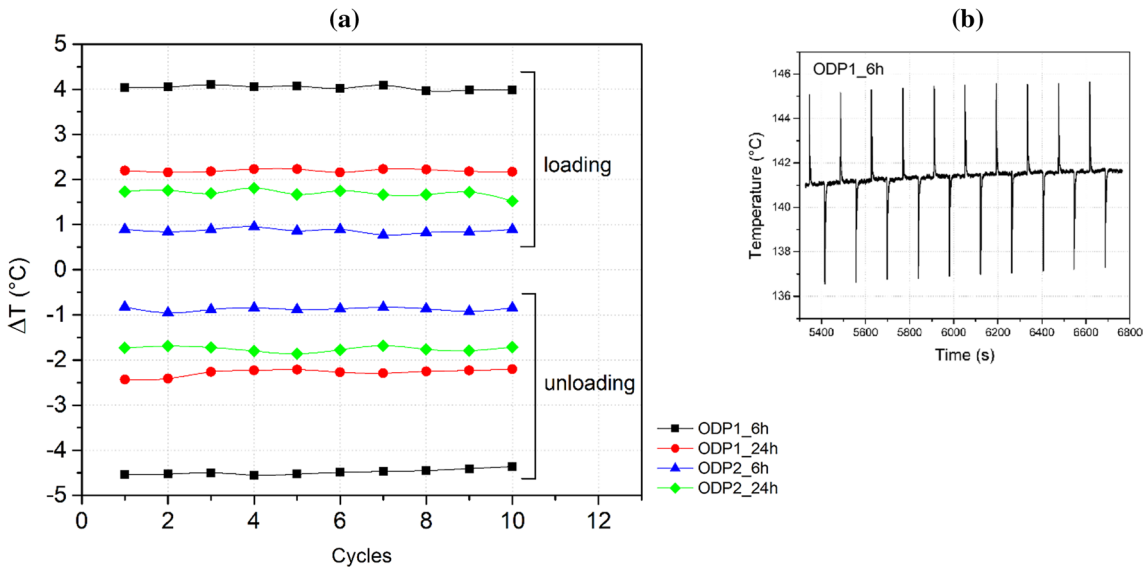

Figure 6 Summary of the cyclic adiabatic ΔT measurements for all the samples at 2.5% of strain and strain rate of 300%/min (**a**) and detail of the temperature profile versus time for ODP1_6h sample (**b**).

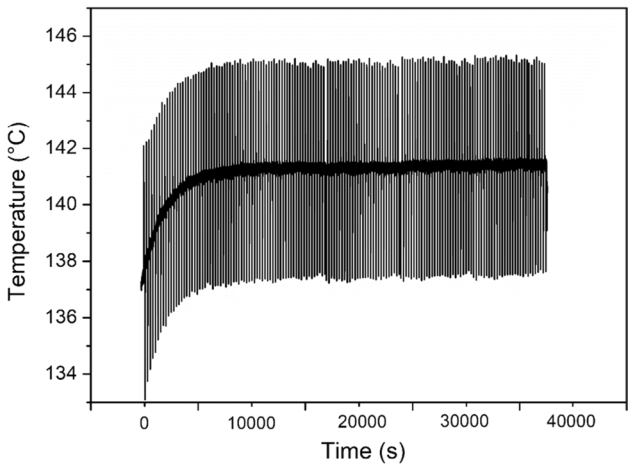

Figure 7 Temperature evolution on ODP1_6h NiMnGa polycrystalline sample during 200 compressive adiabatic cycles.

Table 2 Summary of ΔS and ΔT indirectly evaluated from DSC data and Clausius–Clapeyron relation for sample ODP1_6h and comparison with the experimentally measured ΔT

sample	ΔS–DSC (J Kg^{-1} $°C^{-1}$)	ΔS–CC (J Kg^{-1} $°C^{-1}$)	ΔT–DSC (°C)	ΔT–CC (°C)	ΔT–exp (°C)
ODP1_6h	55,0	31,3	15,4	8,7	4

in Fig. 4 this particular microstructural condition influences the detwinning of martensite, which shows an extremely elastic behavior. Moreover, also the austenite phase is affected by this condition, since the induction of martensite does not occur at quite constant stress values, and the typical flat flag-shape of SMA alloys is not observed. Indeed, the stress induction of martensite is dispersed among a wide range of stresses due to the presence of diffused energy barriers in the sintered alloy. Hence, the austenitic curve does not exhibit a flat plateau but has an almost linear behavior with a very thin hysteresis loop. It is not wrong to highlight that, similarly to strain recovery curves, at low values of strain and stress the recovery goes to negative values of residual strain, as if stored mechanical energy is released by the deformation process, to induce in the sample a recovery which is higher than the induced deformation. The ODP process influences the microstructure improving the mechanical properties and this is noticeable also in the elastic modulus values and in the increment of Clausius–Clapeyron coefficient with respect to the typical one of cast samples. The stored mechanical energy rises the overall mechanical energy levels, particularly concerning the phase transformation.

Considering the elastocaloric performance of the sintered NiMnGa alloy, the samples of series ODP1 give the best results in terms of entropy changes

values, particularly in the heating stage of analysis. In particular, the data for the sample ODP1_6h are better reproducible and more coherent to the increase in the loads applied.

But it is in the elastocaloric investigation in terms of the ΔT generated during adiabatic compression tests, that the promising mechanical properties shown by ODP1_6h give the most interesting results with ΔT values of about 4 °C. In fact, upon 10 cycles of adiabatic deformation it is observed that this sample exhibits the best compromise between mechanical resistance and beneficial grain structure and size to have an ordered martensite induction with a significant thermal effect. Finally, the mechanical response and the related ΔT measured appears to be stable and reliable upon 200 cycles, as has never been found for NiMnGa alloys that usually withstand few cycles.

Finally, considering the comparison between the theoretical and the experimental ΔT, it is important to highlight that the overestimation of the value computed from calorimetric data can be attributed to the assumption that the thermoelastic phenomena occur in adiabatic conditions. On the other hand, in the experimental tests for the direct evaluation of ΔT it is just possible to approach the adiabatic condition by loading the sample extremely rapidly. Indeed, it is possible that partial heat transfer to the environment occurs and the sample is not heated to its full capability. Moreover, the total heat transfer associated with the stress-induced martensitic transformation during experimental mechanical measurements could be affected by the presence of structural defects and energy dispersion. Hence, the microstructural features of the samples could play an important role in the efficiency and homogeneity of the stress-induced TMT with respect to the simply thermally-induced TMT, and, consequently, the registered ΔT could be lowered. Also in the case of the computation from the Clausius–Clapeyron relation derived from the strain recovery curves, the obtained ΔT and ΔS values are higher than the experimental one. In fact, the ΔS is related not only to the thermally induced TMT but also to the contributions of the different degrees of order between twinned and detwinned martensite and elastic deformation. It is probable that the presence of defects, pores and stored energy at the microstructural level affects more significantly the formation of detwinned martensite. Finally, also the actual thermal conductivity of the samples influences the experimentally measured ΔT giving discrepancies with respect to the theoretical point of view.

Conclusions

NiMnGa polycrystalline samples were prepared by open die pressing sintering process, starting from ball milled powders. Different kind of microstructure were developed by four thermomechanical processing routes. After a complete mechanical characterization in compression configuration, all the samples exhibited improved and stronger mechanical performances with respect to cast samples, with higher stresses reached, good strain recovery and significant cycling stability.

For elastocaloric purposes, the best results are reported for sample ODP1 obtained after water quench and thermally treated for 6 h at 925 °C. A stable value of ΔT of about ± 4 °C was measured for the first time for a NiMnGa sample for 200 adiabatic compression cycles, without detection of any degradation or failure.

Acknowledgements

Not applicable.

Author contributions

The authors confirm contribution to the paper as follows. F.V. and E.V. contributed to conceptualization; MT and EV performed formal analysis; FV, MT and EB done investigation; MT done data curation; FV and EV contributed to writing—original draft; FV contributed to writing—review and editing; EV helped in visualization; FP and EV contributed to supervision; FP done project administration.

Funding

Open access funding provided by ICMATE - LECCO within the CRUI-CARE Agreement.

Data availability

The data that support the findings of this study are available from the corresponding author upon reasonable request.

Declarations

Conflict of interest The Authors have no conflict of interest.

References

[1] Takeuchi I, Sandeman K (2015) Solid-state cooling with caloric materials. Phys Today 68(12):48–54

[2] Report of the International Energy Agency (IEA) (2018) The Future of Cooling: opportunities for energy-efficient air conditioning, p 5–88

[3] Moya X, Mathur ND (2020) Caloric materials for cooling and heating. Science 370:797–803

[4] Engelbrecht K (2019) Future prospects for elastocaloric devices. J Phys Energy 1:021001

[5] Greco A, Aprea C, Maiorino A, Masselli C (2019) A review of the state of the art of solid-state caloric cooling processes at room-temperature before 2019. Int J Refrig 106:66–88

[6] Bruederlin F, Bumke L, Chluba C, Ossmer H, Quandt E, Kohl M (2018) Elastocaloric cooling on the miniature scale: a review on materials and device engineering. Energy Technol 6:1588–1604

[7] Cazorla C (2019) Novel mechanocaloric materials for solid-state cooling applications. Appl Phys Rev 6:041316

[8] Tušek J, Engelbrecht K, Mañosa L et al (2016) Understanding the thermodynamic properties of the elastocaloric effect through experimentation and modelling. Shape Mem Superelast 2:317–329

[9] Aaltio I, Fukuda T, Kakeshita T (2019) A perspective on elastocaloric effect in Ti–Ni-based shape memory alloys. Shape Mem Superelast 5:230–234

[10] Manosa L, Planes A (2017) Materials with giant mechanocaloric effects: cooling by strength. Adv Mater 29:1603607

[11] Kirsch SM, Welsch F, Michaelis N, Schmidt M, Wieczorek A, Frenzel J, Eggeler G, Schütze A, Seelecke S (2018) NiTi-based elastocaloric coolingon the macroscale: from basic conceptsto realization. Energy Technol 6:1567–1587

[12] Tušek J, Engelbrecht K, Mikkelsen LP, Pryds N (2015) Elastocaloric effect of Ni-Ti wire for application in a cooling device. J Appl Phys 117(12):124901

[13] Cong D, Xiong W, Planes A, Ren Y, Mañosa L, Cao P, Nie Z, Sun X, Yang Z, Hong X, Wang Y (2019) Colossal elastocaloric effect in ferroelastic Ni-Mn-Ti alloys. Phys Rev Lett 122:255703

[14] Yan H-L, Wang L-D, Liu H-X, Huang X-M, Jia N, Li Z-B, Yang B, Zhang Y-D, Esling C, Zhao X (2019) Giant elastocaloric effect and exceptional mechanical properties in an all-d-metal Ni–Mn–Ti alloy: experimental and ab-initio studies. Mater Des 184:108180

[15] Mendonça AA, Jurado JF, Stuard SJ, Silva LEL, Eslava GG, Cohen LF, Ghivelder L, Gomes AM (2018) Giant magnetic-field-induced strain in Ni_2MnGa-based polycrystal. J Alloy Compd 738:509–514

[16] Chernenko VA, L'vov VA (2008) Magnetoelastic nature of ferromagnetic shape memory effect. Mater Sci Forum 583:1–20

[17] Albertini F, Solzi M, Paoluzi A, Righi L (2008) Magnetocaloric properties and magnetic anisotropy by tailoring phase transitions in NiMnGa alloys. Mater Sci Forum 583:169–196

[18] Villa E, Tomasi C, Nespoli A, Passaretti F, Lamura G, Canepa FJ (2020) Investigation of microstructural influence on entropy change in magnetocaloric polycrystalline samples of NiMnGaCu ferromagnetic shape memory alloy. Mater Res Technol 9:2259–2266

[19] Qu YH, Cong DY, Li SH, Gui WY, Nie ZH, Zhang MH, Ren Y, Wang YD (2018) Simultaneously achieved large reversible elastocaloric and magnetocaloric effects and their coupling in a magnetic shape memory alloy. Acta Mater 151:41–55

[20] Gracia-Condal A, Planes A, Manosa L, Wei Z, Guo J, Soto-Parra D, Liu J (2022) Magnetic and structural entropy

contributions to the multicaloric effects in Ni-Mn-Ga-Cu. Phys Rev Mater 6:084403

[21] Villa F, Nespoli A, Fanciulli C, Passaretti F, Villa E (2020) Physical characterization of sintered NiMnGa ferromagnetic shape memory alloy. Materials 13(21):4806

[22] Villa F, Morlotti A, Fanciulli C, Passaretti F, Albertini F, Villa E (2023) Anomalous mechanical behavior in NiMnGa alloy sintered through open die pressing method. Mater Today Commun 34:105391

[23] Bonnot E, Romero R, Manosa L, Vives E, Planes A (2008) Elastocaloric effect associated with the martensitic transition in shape-memory alloys. Phys Rev Lett 100:125901

[24] Chernenko VA, Villa E, Salazar D, Barandiaran JM (2016) Large tensile superelasticity from intermartensitic transformations in $Ni_{49}Mn_{28}Ga_{23}$ single crystal. Appl Phys Lett 108(7):071903

[25] Villa F, Bestetti E, Frigerio R, Caimi M, Tomasi C, Passaretti F, Villa E (2022) Elastocaloric properties of polycrystalline samples of NiMnGaCu ferromagnetic shape memory alloy under compression: effect of improvement of thermoelastic martensitic transformation. Materials 15:7123

[26] Pataky GJ, Ertekin E, Sehitoglu H (2015) Elastocaloric cooling potential of NiTi, Ni_2FeGa, and CoNiAl. Acta Mater 96:420–427

[27] Huang YJ, Hu QD, Bruno NM, Chen J-H, Karaman I, Ross JH, Jr., Li JG (2015) Giant elastocaloric effect in directionally solidified Ni–Mn–In magnetic shape memory alloy. Scr Mater 105:42–45

[28] Álvarez-Alonso P, Aguilar-Ortiz CO, Villa E, Nespoli A, Flores-Zúñiga H, Chernenko VA (2017) Conventional and inverse elastocaloric effect in Ni-Fe-Ga and Ni-Mn-Sn ribbons. Scr Mater 128:36–40

[29] Wójcik A, Aguilar-Ortiz C, Maziarz W, Szczerba MJ, Sikora M, Żywczak A, Álvarez-Alonso P, Villa E, Flores-Zúñiga H, Cesari E, Chernenko VA (2017) Transformation behavior and inverse caloric effects in magnetic shape memory $Ni_{44-x}Cu_xCo_6Mn_{39}Sn_{11}$ ribbons. J Alloy Compd 721:172–181